Progress In Electromagnetics Research C, Vol. 69, 159–167, 2016

AMC-Integrated Reconfigurable Beamforming Folded Dipole Antenna with Parasitic and RF MEMS

Herwansyah Lago[1], Mohd F. Jamlos[1, 2, *], Ping J. Soh[1, 3], and Guy A. E. Vandenbosch[3]

Abstract—A beam-reconfigurable printed antenna on an Artificial Magnetic Conductor (AMC) is proposed for navigation and radiolocation applications at a frequency of 9.41 GHz. The AMC is formed based on a periodic Jerusalem cross shaped slot structure and is located in between two substrate layers, close to the radiator. The AMC plane has a bandwidth of 1.95 GHz around the targeted frequency of 9.41 GHz. By integrating micro-electro-mechanical system (MEMS) switches on the folded patches in combination with parasitic elements, a beam steering capability of up to $\pm 58^\circ$ is achieved with a rear full ground plane. This eliminates the need for a mechanical steering system, which is traditional in the applications targeted. The antenna achieves a high gain of 8.08 dBi and 90% efficiency. A good agreement between simulated and measured results is obtained.

1. INTRODUCTION

The capability of beam modification in antennas to suit various applications has long been investigated by various researchers. The benefit of such feature is clear: it enables efficient power utilization at the transceiver along with increased coverage and transmission distance extension. However, the antenna design process to achieve reconfigurability is challenging. Conventional options include the use of mechanical elements [1], controlling surface currents using parasitics or switches [2–9], and controlling the phase fed into individual elements of the array [10].

More recent and innovative methods incorporate the use of metasurfaces [1, 11]. Recently, several two-dimensional (2-D) printed metasurfaces have been presented: the high impedance surface (HIS) [11], the electromagnetic band-gap (EBG) ground plane [12, 13], the reactive impedance substrate (RIS) [14], and the artificial magnetic conductor (AMC) [15–20]. The AMC structure is a periodic structure with special electromagnetic properties, potentially used as HIS or PMC. One of AMC's main attractive features is that it can be placed in close proximity of radiators such as planar dipoles or monopoles, to enable a low profile structure [15]. Besides that, it may also help in antenna miniaturization while improving bandwidth [14]. Moreover, surface waves are suppressed due to the near-zero phase difference between the incident and reflected waves, resulting in improved directivity and antenna front-to-back ratio (FBR). For example, a high gain directional folded dipole was proposed using a metasurface in [21]. The acceptable bandwidth of an AMC is in the range of $\pm 90^\circ$ as reported in [15–17].

A popular method to enable radiation pattern reconfiguration is via PIN diodes [21, 22]. This option may also be combined with other beam-tuning methods such as HIS and parasitic tuning to enhance beam-reconfigurability, as demonstrated on a quasi-yagi-uda antenna in [11]. Despite this, the presence of PIN diodes typically results in reduced antenna efficiency due to the passive nature [21]. This consequently affects the antenna gain [23]. Moreover, the applicability of PIN diodes is also limited in terms of insertion loss, isolation, power handling capability and frequency. Micro-electro-mechanical

Received 24 August 2016, Accepted 7 November 2016, Scheduled 22 November 2016

* Corresponding author: Mohd Faizal Jamlos (mohdfaizaljamlos@gmail.com).

[1] Advanced Communication Engineering Centre (ACE), School of Computer & Communication Engineering, Universiti Malaysia Perlis, Malaysia. [2] Faculty of Mechanical Engineering, Universiti Malaysia Pahang, Pekan, Malaysia. [3] ESAT-TELEMIC Research Division, Department of Electrical Engineering, Katholieke Universiteit Leuven, Kasteelpark Arenberg 10, Leuven 3001, Belgium.

systems (MEMS) have been proposed in [24] as a better alternative due to their improved power handling capability, isolation and insertion losses at high frequency compared to PIN diodes [5, 7, 25–27].

This work presents, to the best of our knowledge for the first time, a metasurface-incorporated antenna integrated with parasitic and MEMS switches to effectively enable a wide beam reconfigurable radiation pattern. The proposed antenna is capable of a wide beam steering of $\pm 58^\circ$ without reduction of the conductor backing by a full ground plane. The high gain is maintained via the combined use of the MEMS, parasitics, and AMC structures. The proposed antenna is designed to operate at the frequency of 9.41 GHz (X-band) due to its allocation for ranging and detection system applications [33]. The organization of the paper is as follows. The structure and characteristics of the AMC plane are first introduced in Section 2. Next, the AMC plane and dipole integration procedures are discussed in Section 3. Finally, the performance of the overall antenna structure incorporating the parasitic elements is examined prior to the concluding remarks.

2. AMC DESIGN

The AMC design procedure is based on determining the phase and magnitude response of an infinite array of unit cells. The target is a lossless AMC at the resonant frequency of 9.41 GHz, with 0° reflection phase and 0 dB reflection coefficient for an incident plane wave. The bandwidth of the AMC is defined as the $\pm 90^\circ$ in-phase band [16, 19].

Figure 1 depicts the topology. The AMC plane is placed in between two layers of Taconic TLY-5 substrate, which features a thickness, dielectric constant (ε_r) and loss tangent ($\tan\delta$) of 1.5748 mm, 2.2 and 0.006, respectively. The ground plane is located below the AMC. Conventionally, square patches are chosen to form the AMC unit cell [15, 27]. However, in this work, the proposed unit cell structure incorporates a Jerusalem Cross (JC) slot centered in the patch. The result is a considerable reduction of the dimensions of the unit cell, from ca. 0.5λ to $0.15 \times 0.15\lambda$ ($5 \times 5\,\text{mm}^2$). The EM field of the proposed AMC structure can be represented by the equivalent circuit as in Fig. 1(c) as discussed in Ref. [32]. The conducting element of the AMC design is determined as the inductance while the gap in between the adjacent conducting elements provides the capacitance. The simulated phase response and reflection magnitude shown in Fig. 2 clearly indicate that the AMC exhibits a PMC-like characteristic with a 0° phase response at 9.41 GHz and with a bandwidth of 1950 MHz. Simulations were performed using CST Microwave Studio with unit cell boundaries and Floquet ports to mimic the infinite planar periodicity.

To properly evaluate the effect of the AMC plane in this specific layer configuration, two simple rectangular microstrip antennas were designed, one with and one without AMC. The same substrates are used, and the radiating patches are designed to operate at 9.41 GHz, resulting in a size of 11 mm × 10.5 mm for the case without AMC and a size of 5 mm × 4 mm for the case with AMC.

A full ground plane is placed on the bottom-most layer in both cases. Fig. 3 compares the performance of the proposed AMC-based antenna and the reference antenna. The −10 dB impedance bandwidth is about 5.4% for the case with AMC compared to 4% for the case without AMC. Further, the use of the AMC plane results in a much higher 8.17 dBi peak gain compared to a peak gain of 6.14 dBi for the case without AMC. Note also the higher maximum total efficiency of the AMC-based antenna (93%) compared to the case without AMC (90%).

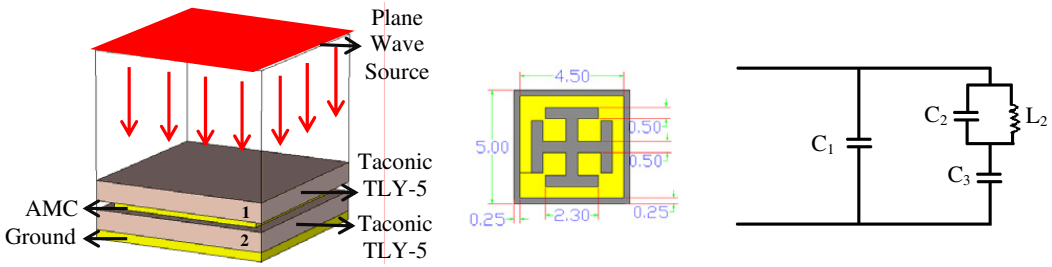

Figure 1. AMC (a) layer structure, (b) unit cell (units in mm), and equivalent circuit.

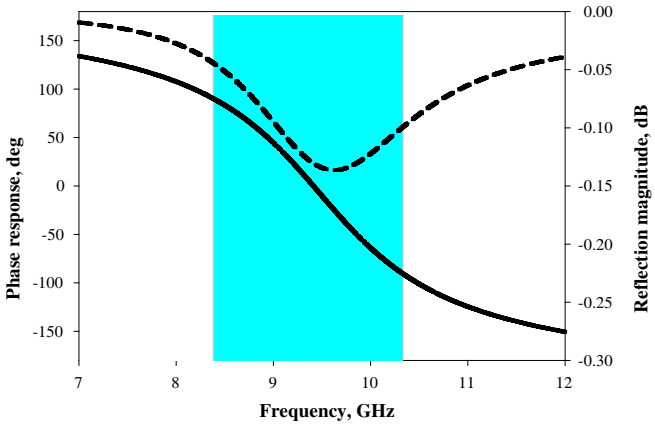

Figure 2. Reflection magnitude (dashed line) and phase response (solid line) of the AMC plane.

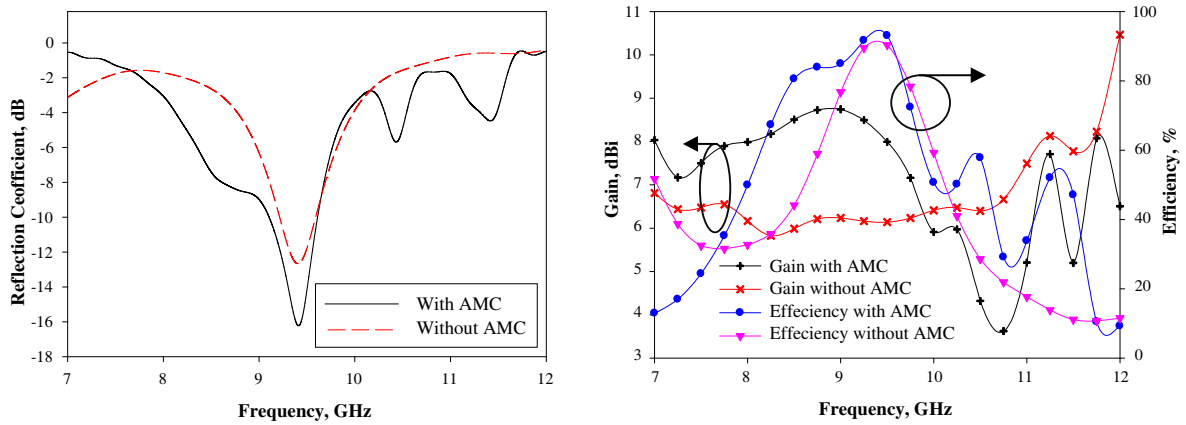

Figure 3. Simulated (a) reflection coefficient and (b) gain and total efficiency of the simple rectangular microstrip antennas without and with AMC.

3. AMC-INTEGRATED RECONFIGURABLE FOLDED DIPOLE ANTENNA (ARFD)

The AMC-integrated reconfigurable folded dipole (ARFD) antenna depicted in Fig. 4 consists of the four layers as depicted in Fig. 4(a), and a metal layer forming the E-folded dipole structure on top (see Fig. 4(b)). The structure is initially designed using the dipole concept as suggested in [31] which resulted in an overall length of 29.6 mm ($\sim 1\lambda$ at 9.41 GHz). The arms are folded for size compactness. The lengths of the first, second, and third fold are (6 mm) 0.19λ, (4.5 mm) 0.14λ, and (3.5 mm) 0.11λ, respectively. Each subsequent fold is shortened by about 25% in order to enable the efficient placement of the folded arms in a quasi-spiral structure. The AMC is formed by 9×3 unit cells as defined in Fig. 4(c).

The structure is fed via a 50 Ω of SMA coaxial probe feed located at the center of the $5 \times 5\text{mm}^2$ square shape. This shape is functional as the platform to distribute the energy to the folded dipole through the transmission feeding line at it's both side where each line has a width of 2 mm. Two RF MEMS101 switches are placed onto the feeding lines at 5.5 mm from the center, which enables pattern reconfigurability. As illustrated in Fig. 5, obviously the symmetry of the topology for both switch configurations results in a corresponding symmetry for the antenna characteristics. It is clearly shown that the antenna is operational in the targeted frequency band. The maximum gain is 6.4 dBi and the efficiency 90%. The beam tilt directions reach a modest $\pm 20^\circ$ as shown in Fig. 5(b). Fig. 5(c) shows the z component of the electric field at the resonant frequency upon the activation of the right MEMS.

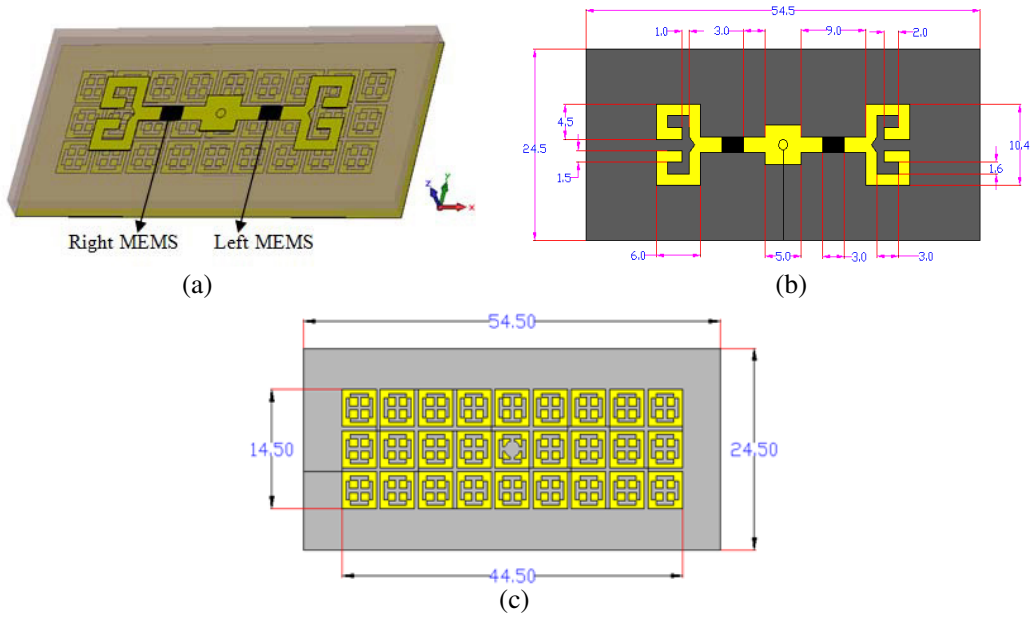

Figure 4. Topology of the proposed antenna (units in mm). (a) 3-D view, (b) top view, (c) AMC plane [30].

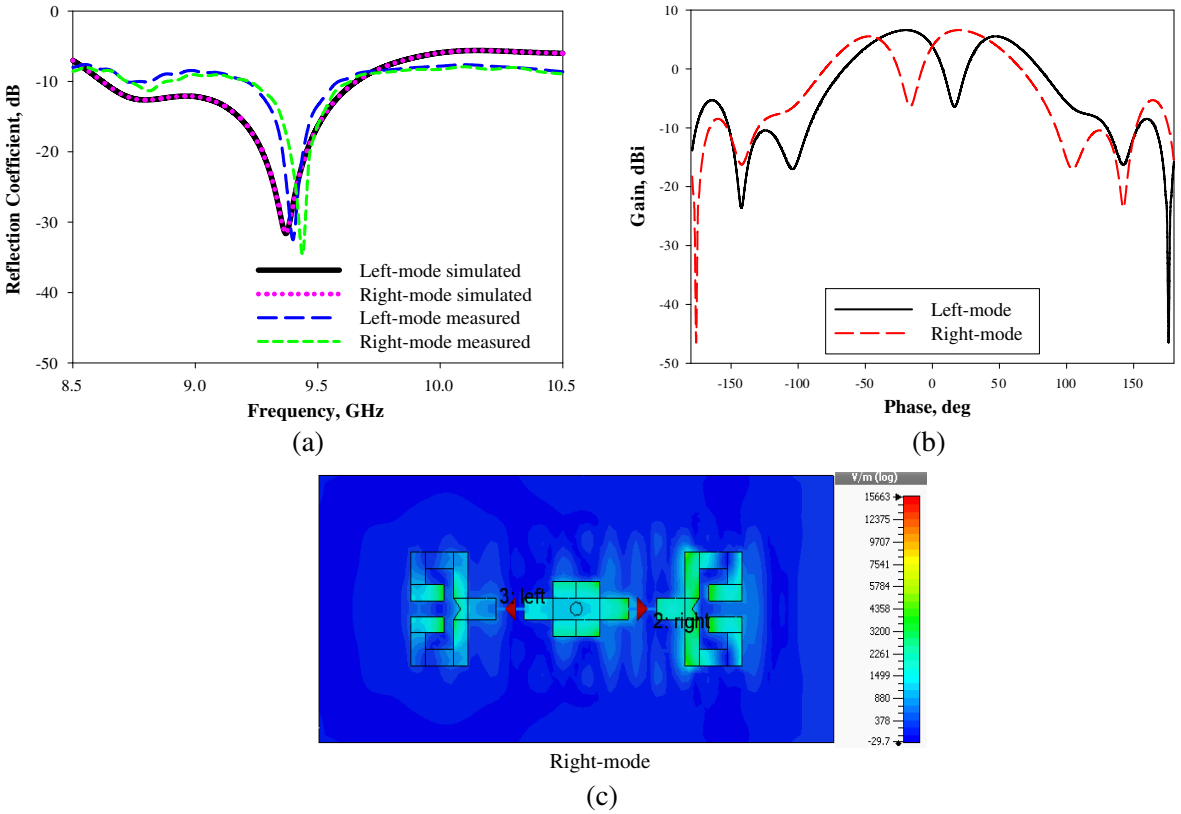

Figure 5. (a) The topology of the AMC based folded dipole antenna loaded with T-shaped parasitic, ARFD-P, units in mm and (b) simulated z-component of electric field for the right element activated at 9.41 GHz.

It can be seen that the current fed via the centered SMA connector is well fed into the activated dipole element.

4. AMC-INTEGRATED RECONFIGURABLE FOLDED DIPOLE ANTENNA WITH PARASITIC (ARFD-P)

Improvised version of ARFD antenna design has been realized by adding T-shaped parasitic elements located near the radiating elements, see Fig. 6(a). This structure is referred to as the AMC-integrated reconfigurable folded dipole with parasitic elements (ARFD-P). The T-shaped parasitic elements are designed with an approximate length of 0.2λ for the two vertical (y-axis) arms and 0.16λ for the horizontal (x-axis) arm. These parasitic elements which are located 0.05λ from the dipole act as a beam director, similar as in a Yagi-Uda antenna [29] where their presence influences the gain and main lobe direction. In this paper, it is found that the T-shaped parasitic elements have tilted the main beam towards the end fire direction, resulting in an impressive increment of the tilt angle to $+-58$ compared to the ARFD, as illustrated in Fig. 9(b). From the current distribution depicted in Fig. 6(b), it can be concluded that the mutual coupling between the elements in the ARFD-P is higher than in the ARFD and contributes considerably to the characteristics of the radiation pattern.

The fabricated prototype of proposed ARFD-P antenna is shown in Fig. 7. The switches have been integrated to the antenna by using bond wire as elaborated in Refs. [5, 24]. All measurement processes have been carried out in Advanced Communication Engineering Centre (ACE) of Universiti Malaysia Perlis (UniMAP) with the help of Anechoic Chamber using the E8051C Network Analyzer and DAMS 5000 measurement system as shown in Fig. 8. Horn antenna performs as a transmitter and antenna under test (AUT) act as a receiver. Both are separated by a distance about 1.2 m apart. The horn is competent to function from 1 GHz to 18 GHz. The gates of the MEMS switches are injected with 90 V (DC) and 0 V (DC) for switch activation and deactivation during measurement.

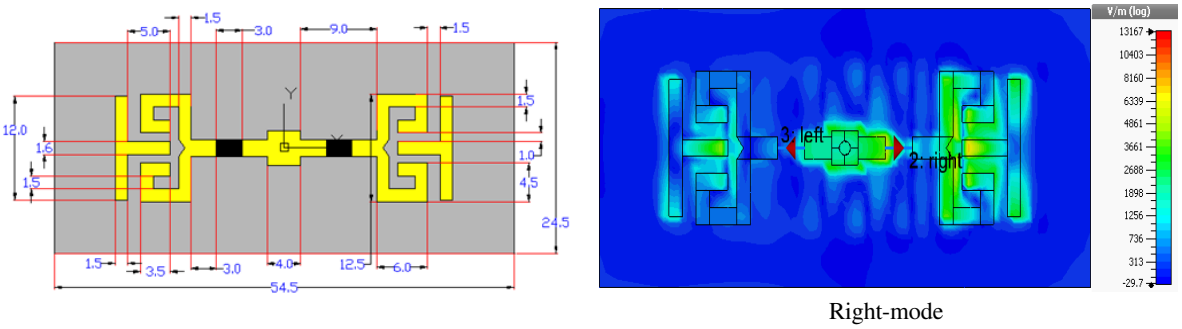

(a) (b)

Figure 6. (a) The topology of the AMC based folded dipole antenna loaded with T-shaped parasitic, ARFD-P, units in mm and (b) simulated z-component of electric field for the right element activated at 9.41 GHz.

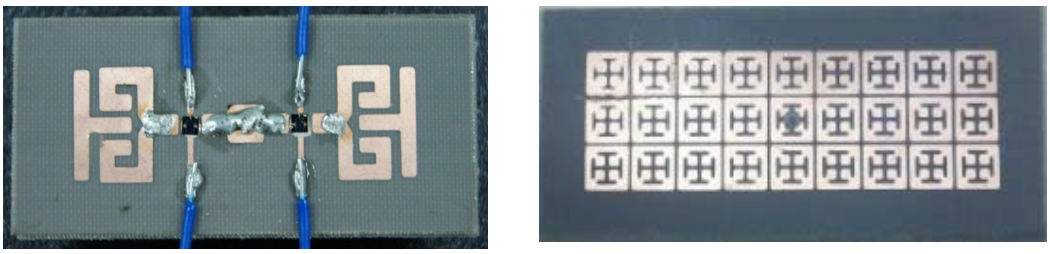

(a) (b)

Figure 7. Photographs of the manufactured (a) ARFD-P structure and (b) AMC plane.

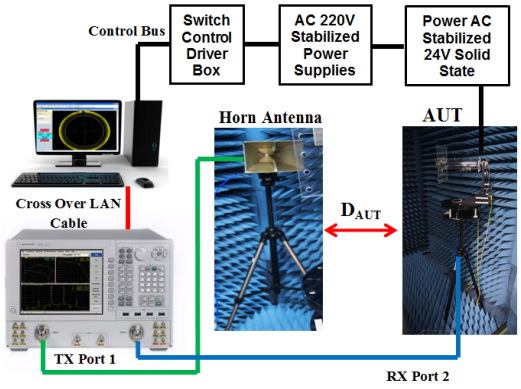

Figure 8. Antenna measurement setup.

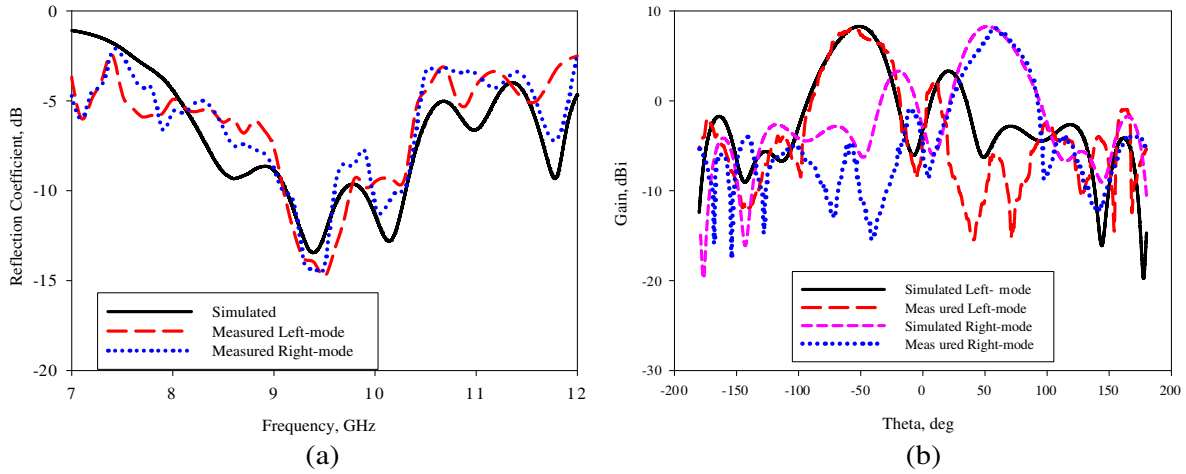

Figure 9. Simulated and measured (a) reflection coefficients of the ARFD-P and (b) radiation patterns (cartesian) for two modes of the ARFD-P at 9.41 GHz.

The measured and simulated reflection coefficients are illustrated in Fig. 9(a). The results are comparable for both switch configurations. The measurements are slightly higher than the simulations. One obvious reason is the fact that in the simulations a perfect ON and OFF state were used as models for the MEMS switches in the two states. Further, few strip lines (made using copper) introduced on the fabricated antenna as the source connection port to activate and deactivate the switches. This additional strip lines are resulting to these deviations. However, this result is acceptable. As depicted in Fig. 9(b), the measured and simulated radiation patterns are also in good agreement for both switch configurations in the xz-plane. The maximum measured gain for both configurations is about 8.08 dBi at $\pm 58^\circ$ while the simulated gain is 8.27 dBi at $\pm 51^\circ$.

5. COMPARISON WITH STATE-OF-THE-ART

Compared to previously investigated metasurface-based, pattern-reconfigurable antennas, see Table 1, the proposed ARFD-P antenna achieves the highest gain and efficiency, and the largest steerable beam angle without any ground plane reduction. It is also worth noting that, to the best knowledge of the authors, this antenna is the only one which applies RF MEMS switches to realize beam reconfigurablility. By adding parasitic elements on the ARFD-P, the main lobe direction can be steered up to $\pm 58^\circ$ while simultaneously reaching a gain of 8.08 dBi. The ARFD antenna is only steerable by up to $\pm 20^\circ$ in the xz-plane with a gain of 6.4 dBi. These results have been reached by a combined functioning of the AMC plane and the parasitic element as a director.

Table 1. Comparison with previous reported radiation pattern reconfigurable antennas implemented on metasurfaces.

Antenna type	Frequency (GHz)	Electrical size of antenna (width × length × thickness)	Technique to realize beam steering	Maximum gain (dBi)	Steering angle (°)	Bandwidth (%)	Efficiency (%)
Normal circular patch with metasurface [1]	5.5	$70 \times 70 \times 3.05$ mm ($1.28 \times 1.28 \times 0.06\lambda$)	Mechanically	7.2	±32	-	85
Yagi-uda like with HIS [11]	2.4	$120 \times 155 \times 10.5$ mm ($0.96 \times 1.24 \times 0.08\lambda$)	Pin Diode	4.12	−40	-	58
				4.34	50		62
Yagi-uda with EBG [28]	0.562	$630 \times 630 \times 55$ mm ($1.18 \times 1.18 \times 0.1\lambda$)	SPDT and Pin Diode	5.27	45	-	53.30
				5.14	135		
				5.1	225		
				5.01	315		
Branched radiators with AMC and tunable power divider [29]	2.4	$100 \times 100 \times 10$ mm ($0.8 \times 0.8 \times 0.08\lambda$)	Pin Diode	3.28	40	-	-
				6.62			
Proposed ARFD [30]	9.41	$54.5 \times 24.5 \times 3.25$ mm ($1.71 \times 0.77 \times 0.1\lambda$)	MEMS	6.4	±20	10.56	90
Proposed ARFD-P	9.41	$54.5 \times 24.5 \times 3.25$ mm ($1.71 \times 0.77 \times 0.1\lambda$)	MEMS	8.08	±58	5.94	90

6. CONCLUSIONS

In this work, an AMC-integrated reconfigurable folded dipole antenna with parasitic elements is proposed and investigated. Its pattern reconfigurability is enabled by the implementation of two RF MEMS switches in the antenna. The AMC plane integrated below the antenna resulted in a higher 8.08 dBi gain and about 90% of simulated efficiency. To enable a wide beam-steerable angle, parasitic elements have been introduced in close proximity to the dipole elements to act as directors. Simulation and measurement results presented are satisfactory in terms of reflection coefficient and radiation pattern properties. The overall antenna structure is validated to enable beam switching of up to ±58° without any truncation of the full ground plane.

REFERENCES

1. Zhu, H. L., S. W. Cheng, and T. I. Yuk, "Mechanically pattern reconfigurable antenna using metasurface," *IEEE Transaction on Antennas and Propagation*, Vol. 9, 1331–1336, 2015.
2. Edalati, A. and T. A. Denidni, "Frequency selective surface for beam-switching application," *IEEE Transaction on Antennas and Propagation*, Vol. 61, 195–200, 2013.
3. Rodrigo, D., B. A. Cetiner, and L. Jofre, "Frequency, radiation pattern and polarization reconfigurable antenna using a parasitic pixel layer," *IEEE Transaction on Antennas and Propagation*, Vol. 62, 3422–3427, 2014.

4. Pringle, L. N., P. H. Harms, S. P. Blalock, G. N. Kiesel, E. J. Kuster, P. G. Friederich, R. J. Prado, J. M. Lorris, and G. S. Smith, "A reconfigurable aperture antenna based on switched links between electrically small metallic patches," *IEEE Transaction on Antennas and Propagation*, Vol. 52, 1434–1445, 2004.
5. Kovitz, J. M., H. Rajagopalan, and Y. Rahmat-Samii, "Design and implementation of broadband MEMS RHCP/LHCP reconfigurable arrays using rotated E-shaped patch elements," *IEEE Transaction on Antennas and Propagation*, Vol. 63, 2497–2507, 2015.
6. Gianvittorio, J. P. and Y. Rahmat-Samii, "Reconfigurable patch antennas for steerable reflectarray applications," *IEEE Transaction on Antennas and Propagation*, Vol. 54, 1388–1392, 2006.
7. Petit, L., L. Dussopt, and J.-M. Laheurte, "MEMS-switched parasitic -antenna array for radiation pattern diversity," *IEEE Transaction on Antennas and Propagation*, Vol. 54, 2634–2631, 2006.
8. Qin, P.-Y., Y. J. Guo, and C. Ding, "A beam switching quasi-Yagi dipole antenna," *IEEE Transaction on Antennas and Propagation*, Vol. 6, 4891–4899, 2013.
9. Donelli, M., R. Azaro, L. Fimognari, and A. Massa, "A planer electronically reconfigurable Wi-Fi band antenna based on a parasitic microstrip structure," *IEEE Antennas Wireless Propagation Letter*, Vol. 6, 623–626, 2007.
10. Ding, C., Y. J Guo, P. -Y. Qin, T. S. Bird, and Y. Yang, "A defected microstrip structure (DMS)-based phase shifter and its application to beamforming antenna," *IEEE Transaction on Antennas and Propagation*, Vol. 62, 641–651, 2014.
11. Li, M., S.-Q. Xiao, Z. Wang, and B.-Z. Wang, "Compact surface-wave assisted beam-steerable antenna based on HIS," *IEEE Transaction on Antennas and Propagation*, Vol. 62, 3511–3519, 2014.
12. Akhoondzadeh-Asl, L., D. J. Kern, P. S. Hall, and D. H. Werner, "Wide-bands dipoles on electromagnetic bandgap ground planes," *IEEE Transaction on Antennas and Propagation*, Vol. 55, 2426–2434, 2007.
13. Zhu, S. and R. Langley, "Dual-band wearable textile antenna on an EBG substrate," *IEEE Transaction on Antennas and Propagation*, Vol. 57, 926–935, 2009.
14. Mosallaei, H. and K. Sarabandi, "Antenna miniturization and bandwidth enhancement using a reactive impedance substrate," *IEEE Transaction on Antennas and Propagation*, Vol. 52, 2403–2414, 2004.
15. Yan, S., P. J. Soh, and G. A. E. Vandenbosch, "Low-profile dual-band textile antenna with artificial magnetic conductor plane," *IEEE Transaction on Antennas and Propagation*, Vol. 62, 6487–6490, 2014.
16. Cook, B. S. and A. Shamim, "Utilizing wideband AMC strucutre for high-gain inkjet-printed antennas on lossy paper substrate," *IEEE Antennas Wireless Propagation Letter*, Vol. 12, 76–79, 2013.
17. Joubert, J., J. C. Vardaxoglou, W. G. Whittow, and J. W. Odendaal, "CPW-fed cavity-backed slot radiator loaded with an AMC reflector," *IEEE Transaction on Antennas and Propagation*, Vol. 60, 735–742, 2012.
18. Abbasi, N. A. and R. J. Langley, "Multiband-integrated antenna/artificial magnetic conductor," *IET Microwave Antennas Propagation*, Vol. 5, 711–717, 2011.
19. Yang, W. C., H. Wang, W. Q. che, Y. Huang, and J. Wang, "High-gain and low-loss millimeter-wave LTCC antenna array using artificial magnetic conductor structure," *IEEE Transaction on Antennas and Propagation*, Vol. 63, 390–395, 2015.
20. Folayan, O. and R. Langley, "Dual frequency band antenna combined with a high impedance band gap surface," *IET Microwave Antennas Propagation*, Vol. 3, 1118–1126, 2009.
21. Ren, J., X. Yang, J. Yin, and Y. Yin, "A novel antenna with reconfigurable patterns using H-shaped structures," *IEEE Antennas Wireless and Propagation Letter*, Vol. 14, 915–918, 2015.
22. Kang, W., K. H. Ko, and K. Kim, "A compact beam reconfigurable antenna for symmetric beam switching," *Progress In Electromagnetics Research*, Vol. 129, 1–16, 2012.

23. Bai, Y.-Y., S. Xiao, C. Liu, X. Shuai, and B.-Z. Wang, "Design of pattern reconfgurable antennas based on a two-element dipole array model," *IEEE Transaction on Antennas and Propagation*, Vol. 61, 4867–4871, 2013.
24. Huff, G. H. and J. T. Bernnhard, "Integration of packaged RF MEMS switch with radiation pattern reconfigurable square spiral microstrip antennas," *IEEE Transaction on Antennas and Propagation*, Vol. 54, 464–469, 2006.
25. Safari, M., C. Shafai, and L. Shafai, "X-band tunable frequency selective surface using MEMS capacitive loads," *IEEE Transaction on Antennas and Propagation*, Vol. 63, 1014–1021, 2015.
26. http://www.radantmems.com.
27. Qin, P.-Y., Y. J. Guo, A. R. Weily, and C.-H. Liang, "A pattern reconfigurable U-slot antenna and its application in MIMO system," *IEEE Transaction on Antennas and Propagation*, Vol. 60, 516–528, 2012.
28. Kittiyanpunya, C. and M. Krairiksh, "A four-beam pattern reconfigurable Yagi-Uda antenna," *IEEE Transaction on Antennas and Propagation*, Vol. 61, 6210–6214, 2013.
29. Kim, K., K. Hwang, J. Ahn, and Y. Yoon, "Pattern reconfigurable antenna for wireless sensor network system," *Electronic Letter*, Vol. 48, 984–985, 2012.
30. Lago, H., M. F. Jamlos, N. Bahari, and M. R. Hamid, "Reconfigurable beam pattern folded dipole antenna based on AMC structure," *IEEE International RF and Microwave Conference (RFM)*, 14–16, Kucing, Sarawak, Dec. 2015.
31. Vallecchi, A., J. R. De Luis, F. Capolino, and F. De Flaviis, "Low profile fully planar folded dipole antenna on a high impedance surface," *IEEE Transaction on Antennas and Propagation*, Vol. 60, 51–62, 2014.
32. Liu, X. Y., Y. H. Di, H. Lui, Z. T. Wu, and M. M. Tentzeris, "A planar windmill-like broadband antenna equipped with artificial magnetic conductor for off-body communications," *IEEE Antennas and Wireless Propagation Letters*, Vol. 15, 64–67, 2016.
33. Meloui, M. and M. Essaaidi, "A dual ultra wide band slotted antenna for C and X bands application," *Progress in Electromagnetics Research Letters*, Vol. 47, 91–96, 2014.